THE 11th INTERNATIONAL SYMPOSIUM ON ADVANCED TOPICS IN ELECTRICAL ENGINEERING
March 28-30, 2019
Bucharest, Romania

Numerical Analysis of a Hybrid Stepper Motor for the Electromagnetic Torque Calculation

Ioana Ionică[1,2], Mircea Modreanu[1], Alexandru Morega[2], *Member IEEE*, Cristian Boboc[1]
[1]Icpe
[2]University Politehnica of Bucharest, Faculty of Electrical Engineering
ioana.messico@icpe.ro, mircea.messico@icpe.ro, alexandru.morega@upb.ro, cristianboboc.messico@icpe.ro

***Abstract*- The design of a hybrid stepper motor for achieving a specific performance requires its adequate geometrical sizing that may be performed through numerical modeling. With this aim, the current study documents several aspects of the three–dimensional numerical modeling that was used to predetermine the holding torque for a stepper motor and presents different approaching methods used to reduce redundancies. The results for holding torque calculation are compared with experimental measurements in order to validate the numerical model. Moreover, optimal economic and technical solutions were obtained through successive improvements made in the design phase and concurring to the requirements of the product specification are included.**

***Keywords*: hybrid stepper motor, finite element method, holding torque, mathematical modeling, redundancy, numerical simulation.**

I. INTRODUCTION

The increased demand towards motion control of stepper motors (SMs) play a key role in a wide range of applications demanding for accuracy and repeatability [1].

SMs are increasingly used as digital actuators because they do not require digital–to–analog (D/A) conversion. For instance, SMs are utilized as actuators in a spacecraft instrumentation system [2], or to control drum actuators [3]. Consistently, theoretical and experimental work was devoted to study and compare the SMs with conventional closed–loop positioning systems [4] and to deploy the SMs to a variety of applications.

The SM main parameters are: parasitic torque, holding torque and running torque. Parasitic torque sums up the hysteresis torque, the irreversibility torque and the detent torque.

The SM is largely presented in [5], where a study regarding the detent torque (the torque with the windings not energized) is presented. In SMs, position holding must occur without energy consumption [6–10].

This paper is focused on another important parameter of the SM, namely the holding torque (the torque with the windings energized). Numerical modeling and experimental results are presented and discussed.

II. THE MATHEMATICAL MODEL

A Hybrid SM (HSM) is designed to provide for better efficiency by combining the best features available on both Permanent Magnet and Variable Reluctance stepper motors. The HSM has the advantage of excellent performances regarding the step resolution, torque and speed.

A higher accuracy in the numerical modeling of hybrid SM (HSM), mainly holding torque parameter is the main objective of this work. Therefore, in the design phase all parts of the motor are adequately sized, and the right materials are selected for the hybrid SM volume to be optimal [11-13], using numerical model. Furthermore, redundancy solution (the motor will be equipped with two identical windings – main and redundant) is studied (Fig. 1) in order to maximize SM construction advantages. In the same motor dimensions, the redundant solution (there are two identical sets of windings) will decrease the motor performances, but will increase the reliability of the motor.

Stationary working conditions are considered (no electrical currents in the rotor). The physical model is described by the following particular forms of Maxwell equations [11,14]

magnetic circuit law

$$\nabla \times \mathbf{H} = \mathbf{J}, \tag{1}$$

magnetic flux law

$$\nabla \cdot \mathbf{B} = 0, \tag{2}$$

constitutive law

$$\mathbf{B} = \mu_0 \mu_r \mathbf{H} + \mathbf{B}_r, \tag{3}$$

where, $\mathbf{H}$ [A/m] is the magnetic field strength, $\mathbf{J}$ [A/m^2] is the current density, $\mathbf{B}$ [T] is magnetic flux density, Br [T] is the remanent magnetic flux density (within the permanent magnets), μ_0 [H/m] is magnetic permeability of vacuum, and μ_r is relative magnetic permeability. In view of (2) $\mathbf{B} = \nabla \times \mathbf{A}$, where $\mathbf{A}$ [T/m] is the magnetic vector potential. The boundary condition that closes the computational domain is magnetic insulation, $\mathbf{n}$xrot($\mathbf{A}$) = 0

The coils, with N turns, carry the electrical current I_{coil} [A]. The electrical current density is computed then using

$$J = \frac{N \cdot I_{coil}}{S}, \tag{4}$$

where S [m^2] is the cross–sectional area of the conductor in the coil.

The mathematical model (1)–(4) was solved numerically, using the finite element method (FEM) technique [10].

978-1-7281-0101-9/19/$31.00 ©2019 IEEE

III. The Numerical Modeling of The Hybrid Stepper Motor

The airgap thickness and the magnetic materials of the hybrid SMs have a substantial effect on the motor design [15]. The physical dimensions that influence the design are presented largely in [5,15].

The bi-dimensional models are using simplifying assumptions that affect significantly the results. Therefore, we used three–dimensional models.

A. The Redundancy Solution of HSM

In order to find the suitable redundancy solution for a HSM, two cases, which are different from this point of view, are analyzed.

The HSM in this study has the following constructive elements (Fig. 1): stator stack (1), stator windings (2), one rotor armature and two rotor semi-armatures (3) and two magnets (4). The whole magnetic circuit of the motor was considered. It contains the stator, made of lamination stack of Iron Cobalt and has 8 poles with 10 teeth each, and the rotor that has two semi–armatures and one armature, both made of soft iron and two Samarium – Cobalt PMs between them.

Due to the axial symmetry of the motor, only half of the motor was modeled (Fig. 1).

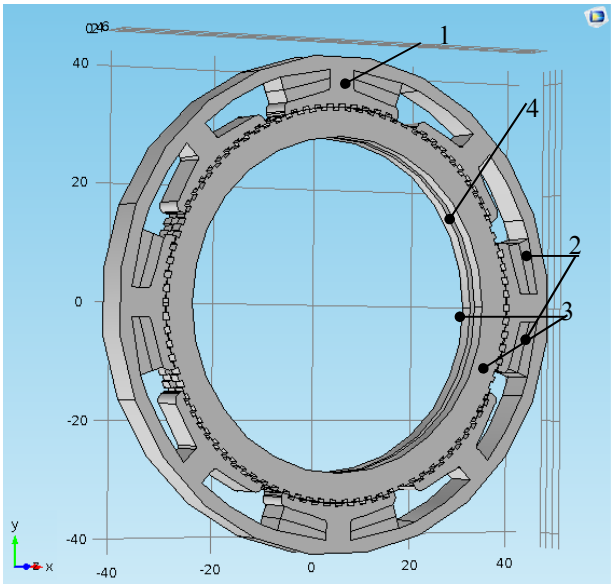

Fig. 1. The hybrid stepper. Dimensions are in millimeters.

The motor has to be configured in two ways, due to his construction with two windings/phase and a redundant winding: as a 2–phase motor (2 half phases in series, 2 half phases in parallel and 1 half–phase as a single phase), and as a 4–phase motor. The switching from 4 to 2 phases is provided at the connector level.

The stator windings that are distributed over the half of the magnetic circuit make the redundancy solution.

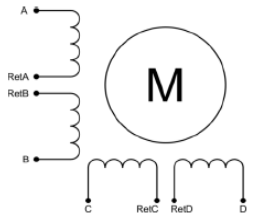

Fig. 2. The hybrid stepper main winding configuration.

The materials used in the numerical modeling and the geometry characteristics of the HSM are presented in Fig. 3.

Geometry characteristics	
Stator	Rotor
Rectangular	Rectangular
t/λ=0.5	t/λ=0.5

Materials	
Stator	Rotor
- Iron Cobalt lamination - Copper for stator windings	- Samarium-Cobalt Permanent Magnets - Magnetic iron

a) The geometry characteristics for the stator and rotor teeth. The materials used in numerical modeling.

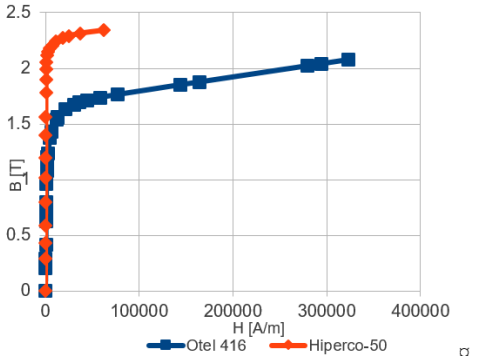

b) The B–H characteristics of the materials for the hybrid stepper.

Fig. 3. The materials and the geometry characteristics of the HSM.

The first solution for redundancy considers the main winding distributed over half of the stator stack and the redundant winding distributed over the other half.

For holding torque calculation, only half of the main winding (Fig. 4), which is distributed over two poles (half distributed over phase configuration), is considered. The other half of the main winding and the redundant winding is not considered in Fig. 4.

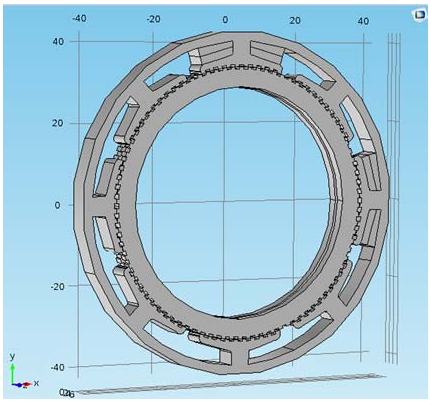

Fig. 4. The constructive elements of the hybrid stepper. Dimensions are in millimeters.

The color map of the magnetic flux density is presented in Fig. 5.

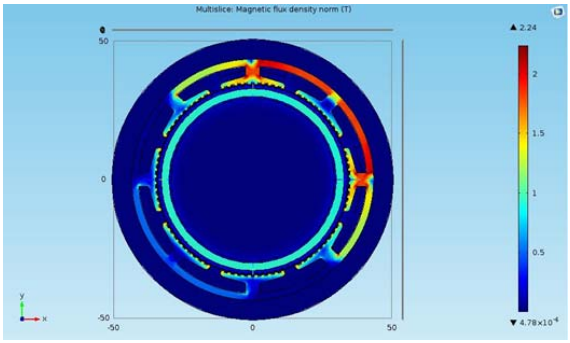

Fig. 5. Magnetic flux density xOy plane.

Fig. 6 presents the ratio between calculated holding torque and required torque (T_n) versus angle characteristic. The maximum relative deviation between the calculated holding torque (T) and the measured experimental model is 17.2%.

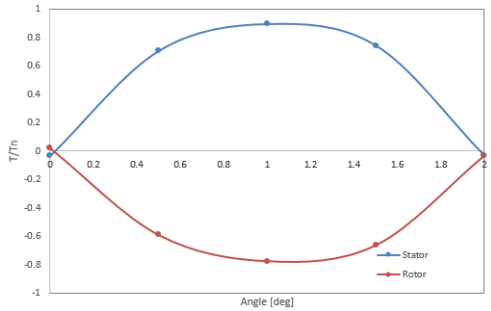

Fig. 6. Calculated holding torque characteristic - Half-phase option, U=26V.

The first solution for redundancy was changed due to some disadvantages, mainly the usage of only half of magnetic circuit. The second solution considers the main winding and the redundant winding distributed over the entire stator stack (Fig. 7). Comparative with Fig. 4, Fig. 7 shows the whole main winding distributed over the entire stator stack. The difference between first and second solution can be seen also in numerical analysis results.

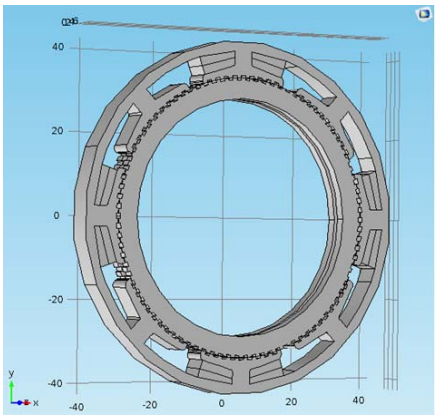

Fig. 7. The constructive elements of the hybrid stepper with the second solution for redundancy. Dimensions are in millimeters.

The magnetic flux density is presented in Fig. 8.

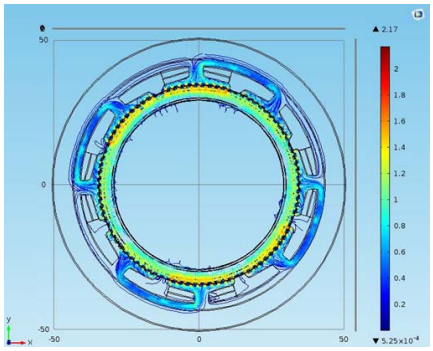

Fig. 8. Magnetic flux density for the half–phase windings configuration.

Fig. 9 presents the ratio between calculated holding torque and required torque (T_n) versus angle characteristic.

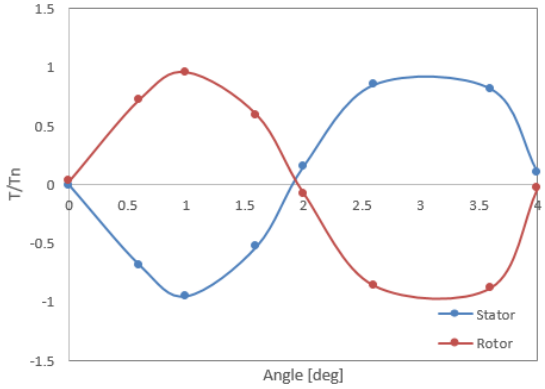

Fig. 9. Calculated holding torque characteristic for half–phase option, $U = 26$ V.

The maximum relative deviation for the computed holding torque as compared with experimental model is 10.7%.

B. The Holding Torque

For the holding torque computation, the winding is supplied, so the magnet and the stator winding are the magnetic field sources. This problem solved formulated assuming a stationary magnetic field. The FEM mesh quality is of a particular concern in the numerical simulations of the HSM because it influences the accuracy of the numerical solution [15]. This is a difficult problem due to airgap

thickness, here 0.1 mm, as compared to the stator outer diameter, here between 60 ÷ 90 mm. The mesh must be adapted to match the required resolution in different motor areas in order to obtain conclusive results.

The HSM here has the following constructive elements (Fig. 9): stator stack (1), stator winding (3), two rotor semi–armatures (2) and one magnet (4). The entire magnetic circuit of the motor was considered in the numerical modeling. It contains the stator (made of lamination stack of Iron Cobalt, and has 8 poles with 10 teeth each) with stator windings (main winding – 3' and redundant winding – 3" distributed on the entire stator stack) and the rotor (has two semi-armatures, both made of Iron Cobalt with an offset of 2 degrees and one Samarium – Cobalt permanent magnet with longitudinal magnetization between them).

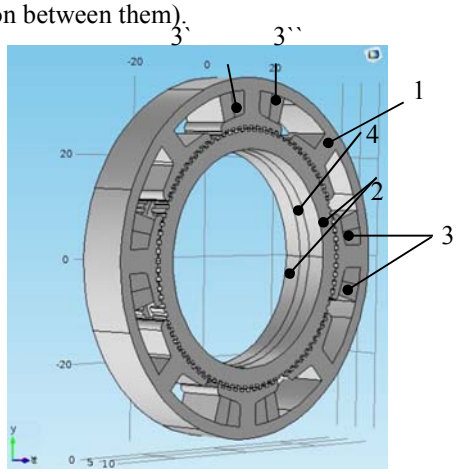

Fig. 10. The hybrid stepper. Dimensions are in millimeters.

The HSM electrical interface is presented in Fig. 11.

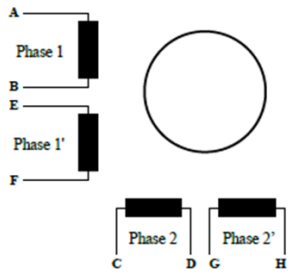

Fig. 11. The hybrid stepper electric interface.

The materials used in the numerical modeling and the geometry characteristics of the SM are presented in Fig. 12.

Geometry characteristics	
Stator	Rotor
Rectangular	Rectangular
t/λ<0.5	t/λ<0.5

BB1 - Materials	
Stator	Rotor
- Iron Cobalt lamination - Copper for Stator windings	- Samarium-Cobalt Permanent Magnet - Iron Cobalt lamination

a) The geometry characteristics for the stator and rotor teeth. The materials used in numerical modeling.

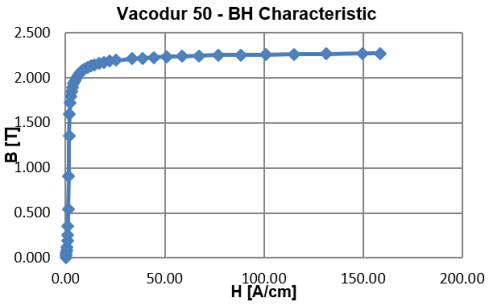

b) The B-H characteristics of the materials for the hybrid stepper.

Fig. 12. The materials and the geometry characteristics of the HSM.

A detail of the magnetic flux density distribution is presented in Fig. 13.

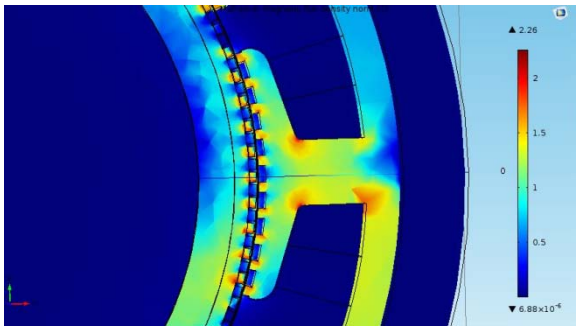

Fig. 13. Detail of Magnetic flux density xOy plane.

Fig. 14 presents the ratio between calculated holding torque and required torque (T_n) versus angle characteristic.

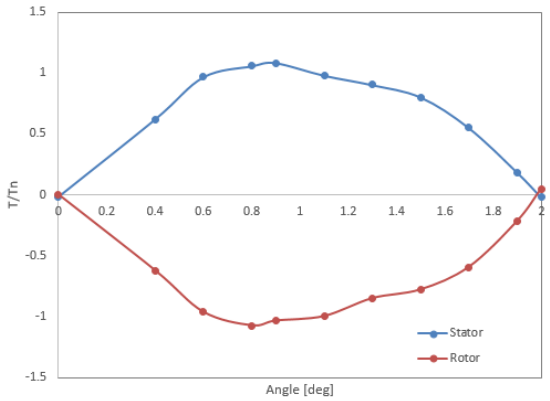

Fig. 14. Holding torque vs angle characteristic.

The maximum relative deviation of the holding torque w.r.t. the experimental model is 19%.

IV. Experimental Results

Verifications were performed on the motor in different powering configuration to establish if the requirements of the technical specifications are fulfilled, and to validate the numerical model. Fig. 15 presents the ratio between holding torque and required torque (T_n) versus angle characteristic.

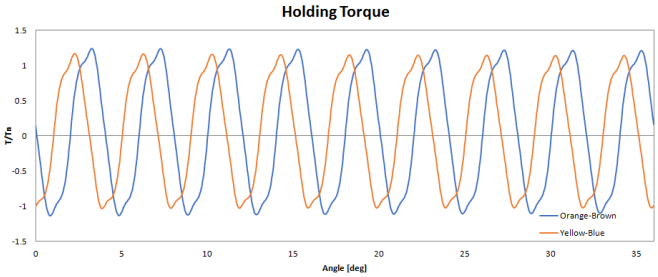

Fig. 15. Holding torque vs angle characteristic, 23.4 V, 36 deg.

Fig. 16 presents the ratio between holding torque and required torque (T_n) versus electrical current characteristic.

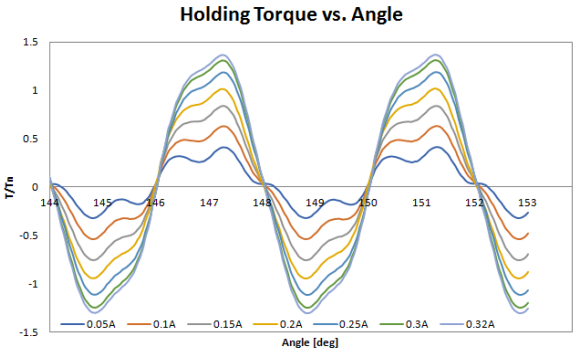

Fig. 16. Holding torque vs angle characteristic for seven different currents.

V. Conclusions

A realistic numerical analysis of HSMs can be realized using three–dimensional models in order to eliminate the simplifying assumptions of the bi-dimensional approximation. Therefore, this paper is concerned with introducing numerical modeling in the design phase of a HSM. Along other parameters, the airgap thickness and the materials influence strongly the HSM design outcome. From the numerical analysis that was conducted outside of this paper, if we increase the HSM airgap with 25%, the torque will decrease with approximately 34%.

Redundancy solution of a SM is studied in order to maximize motor construction advantages. The first solution for redundancy considers the main winding spread on half of the stator stack and the redundant winding distributed over the other half. In the second case, the redundancy solution was changed due to some disadvantages of the first solution, i.e. the use only of half of magnetic circuit The second solution considers the main winding and the redundant winding spread on the entire stator stack.

The holding torque numerical modeling and experimental results are presented.

The deviation values are different for the two redundancy solutions, for the first one is 17.2% and for the second one is 10.7%. Although in the numerical analysis calculation was obtained the same maximum value for holding torque for both variants of redundancy, the breadboards of the stepper motor passed through several measurement methods. Therefore, the measuring methods were improved and the deviation values decrease.

The magnetic flux density reaches the maximum value of 2.3 T, recorded in the stator teeth. Since HSM has a large number of teeth on both the stator and rotor, and a very small airgap, the magnetic saturation in the teeth becomes severe when the flux density in the airgap increases.

Acknowledgment

The authors 1, 2, and 4 acknowledge the financial supported granted by ESA Programme/Project: Electric Motor Spin Into Space – (EMSIS), under the Romanian Industry Incentive Scheme AO/1-7557/. Part of the numerical simulations were conducted in the Laboratory for Multiphysics Modelling at UPB.

References

[1] Proctor, John: Stepping Motors Move In. Product Eng., vol. 34, Feb. 4, 1963, pp. 74-78.
[2] J Nicklas, J. C.: Analysis, Design and Testing of a Position Servo Utilizing a Stepper Motor. Tech. Rep. 32-206, Jet Propulsion Lab., California Inst. Tech., Jan. 25, 1962.
[3] Giles, S.; and Marcus, A. A.: SNAP-8-Control-Drum Actuators. Rep. NAA-SR- 9645, Atomics International, Dec. 15, 1964.
[4] Bailey, S. J. *Incremental Servos. Part I - Stepping vs Stepless Control. Control Eng*., vol. 7, no. 11, Nov. 1960, pp. 123-127; Part 11 - Operation and Analysis, vol. 7, no. 12, Dec. 1960, pp. 97-102; Part III - How They've Been Used, vol. 8, no. 1, Jan. 1961, pp. 85-88; Part IV - Today's Hardware, vol. 8, no. 3, Mar. 1961, pp. 133-135; Part V - Interlocking Steppers, vol. 8, no, 5, May 1961, pp. 116-119.
[5] I. Ionică, M. Modreanu, A. Morega and C. Boboc, "Design and Modeling of a Hybrid Stepper Motor", *2017 10th International Symposium on Advanced Topics in Electrical Engineering (ATEE)*, Bucharest, 2017, pp. 192-195.
[6] https://www.circuitspecialists.com/stepper-motor.
[7] M. Scarpino, A Guide to Steppers, Servos, and Other Electrical Machines, 1st ed., Que, pp.59-61, November 2015.
[8] https://ntrs.nasa.gov/archive/nasa/casi.ntrs.nasa.gov/19690011418.pdf
[9] http://www.nmbtc.com/hybrid-step-motors/
[10] Comsol Multiphysics documentation: http://www.comsol.com/

[11] D. Meeker, Finite Element Method Magnetics, (2009).
[12] J.-M. Jin, "The Finite Element Method in Electromagnetics", John Wiley and Sons Publisher, New York, 2002.
[13] N. M. KHOA, Predicting Electromagnetic Noise in Induction Motors, Master of Science Thesis Stockholm, Sweden 2014.
[14] V. V. Athani Stepper Motors: Fundamentals, Applications And Design, New Age International, 1997.
[15] Holzbecher and H. Si, "Accuracy tests for COMSOL - and Delaunay meshes," in COMSOL Conference, Hannover, 2008.